Published in final edited form as:
Biomed Microdevices. 2014 August ; 16(4): 629–638. doi:10.1007/s10544-014-9865-1.

Planar Microdevices Enhance Transport of Large Molecular Weight Molecules Across Retinal Pigment Epithelial Cells

Jennifer S. Wade and **Tejal A. Desai***
Department of Bioengineering and Therapeutic Sciences, University of California, San Francisco, California 94158, USA

Abstract

Large molecular weight drug delivery to the posterior eye is challenging due to cellular barriers that hinder drug transport. Understanding how to enhance transport across the retinal barrier is important for the design of new drug delivery systems. A novel mechanism to enhance drug transport is the use of geometric properties, which has not been extensively explored in the retina. Planar SU-8/ Poly(ethyleneglycol)dimethacrylate microdevices were constructed using photolithography to deliver FITC dextran across an *in vitro* retinal model. The model consists of retinal pigment epithelial (RPE) cells grown to confluence on transwell inserts, which provides an environment to investigate the influence of geometry on paracellular and transcellular delivery of encapsulated large molecules. Planar microdevices enhanced transport of large molecular weight dextrans across different models of RPE in a size dependent fashion. Increased drug permeation across the RPE was observed with the addition of microdevices as compared to a traditional bolus of FITC dextran. This phenomena was initiated by a non-toxic interaction between the microdevices and the retinal tight junction proteins. Suggesting that increased drug transport occurs via a paracellular pathway. These experiments provide evidence to support the future use of planar unidirectional microdevices for delivery of biologics in ocular applications.

Keywords

Retinal pigment epithelium; Ocular drug delivery; PEGDMA; Microdevices; Biologics

1. Introduction

Age-related macular degeneration, a disease of the posterior eye, is the leading cause of vision loss in adults over the age of 60 in developed nations (Friedman 2004). In the United States, the number of people affected by this disease exceeds 2 million and is expected to double by the year 2020 due to the aging baby boomer population (Friedman 2004). Recent advances in the biotechnology industry have provided patients with highly effective monoclonal antibody and antibody fragment treatments, such as Ranibizumab, for this debilitating disease.

*Corresponding Author: 1700 4th Street, Byers Hall 204, Box 2520, San Francisco, CA 94158, USA Tel.: +1 415 514 4503; Fax: +1 415 514 9656 tejal.desai@ucsf.edu.

Ocular administration of therapeutics is one of the greatest challenges in the field of drug delivery due to the numerous barriers protecting the eye. The standard of care for ocular drug delivery is topical application of liquids or gels. However, this method of administration is not effective in delivering large molecules to the posterior segment of the eye. The limited contact time, distance and limited permeability between the anterior and posterior segments lead to poor absorption and correspondingly low bioavailability of the therapeutic (Barar 2008; Edelhauser et al. 2010; Hornof et al. 2005; Mannermaa et al. 2009; Urtti 2006; Urtti 2005). Additionally, the tight junctions of the retinal pigment epithelium (RPE) and endothelial cells make intravenous delivery of large molecules unrealistic. While low bioavailability at the site of action is a primary concern, off-target effects such as toxicity are also a deterrent to this mode of delivery. As a result, the primary treatment employed to address posterior segment diseases is intravitreal injection (Edelhauser et al. 2010). This highly invasive method can cause complications if conducted erroneously and often results in a lack of patient compliance.

A variety of alternative therapies have been developed to address these challenges; they include implantable drug reservoirs, which must be surgically removed, as well as biodegradable microspheres and thermo-responsive gels to sustain therapeutic drug levels in the eye (Booth et al. 2007; Choonara 2010; Edelhauser et al. 2010; Hamidi et al. 2008; Hiremath and Devi 2010; Mansoor et al. 2009; Paolicelli 2009). In addition, several approaches have examined methods to facilitate the permeability of drugs across cellular barriers, including nanoparticles and permeation enhancers. For example, previous studies in rabbits demonstrated that drug uptake in the cornea is enhanced when nanoparticles with a chitosan coating are employed to deliver a small molecule (Artursson 1996; Dodane 1999; Dornish 2004; Vllasaliu 2010). Researchers have begun to incorporate our existing knowledge of retinal physiology to improve drug delivery (Haghjou et al. 2012; Toda et al. 2011). Recent studies have increased the transport of small molecule drugs by using newly discovered retinal membrane transporters (Kadam et al. 2013; Mannermaa et al. 2006; Nirmal et al. 2013). Receptor-mediated endocytosis has been investigated for the transport of large molecules leveraging the recently discovered neonatal Fc receptor (FcRN) and transferrin receptor (van Bilsen et al. 2011; Daugherty and Mrsny 2006; Kim et al. 2009; Kompella et al. 2013; Kompella et al. 2006; Lin 2009; Thrimawithana et al. 2011; Wadhwa et al. 2009). Unfortunately, these approaches are highly dependent on molecular structure. For example Ranibizumab, an antibody fragment, will not be internalized via FcRN endocytosis due to its missing Fc region. (Chan and Carter 2010; Filpula 2007)

Interest in disrupting barrier function has led to the use of small interfering RNA (siRNA) to target the tight junction proteins claudin and occludin (González-Mariscal et al. 2005; Hanrahan et al. 2012; Johnson et al. 2007). However, use of siRNA *in vivo* is contentious due to concerns about the efficiency of intracellular delivery, reversibility and off-target effects. To date, the effect of device architecture to modulate the retinal barrier, for large molecule drug transport, has not been investigated.

Using established microfabrication techniques, we have developed SU-8/ Poly(ethyleneglycol)dimethacrylate (PEGDMA) planar microdevices, which maximize contact surface area, provide consistent drug volumes and can be used to unidirectionally

deliver large molecule therapeutics. SU-8 was chosen because it is a well-characterized negative photoresist that can easily be patterned into complex structures with specific dimensions. (Anhoj et al. 2006; Mata et al. 2006) PEGDMA is a biocompatible and commonly used hydrogel, which permits the safe encapsulation of a therapeutic and tunable release in the presence of an aqueous solution. (Kumar et al. 2006; Leobandung et al. 2003; Leobandung et al. 2002; Peppas et al. 1999; Ulery et al. 2011)

These devices have previously been successful in delivering small molecules across an intestinal epithelial cell line, specifically human colorectal adenocarcinoma (Caco-2) epithelial cells (Ainslie et al. 2009; Ainslie et al. 2008; Chirra and Desai 2012; Tao and Desai 2003). In this work, we extend our research to the delivery of large molecules across two human retinal pigment epithelial cell types, an adult retinal epithelial cell line (ARPE-19) and fetal retinal epithelial primary cells (hfRPE). ARPE-19 cells have been extensively studied, demonstrate *in vivo* physiological characteristics of retinal tissue, and can be both easily acquired and cultured (Dunn 1996; Maminishkis and Miller 2006; Sonoda 2009). When compared to the broader set of spontaneously immortalized human retinal epithelial cell lines, it is the preferred choice for the aforementioned reasons. However, previous studies have demonstrated that primary cell lines retain more morphological and physiological characteristics than spontaneously immortalized cell lines (Maminishkis and Miller 2006). For this reason a primary culture of hfRPE cells were used to generate an understanding of how well the results from these transport studies would translate to an *in vivo* model. Both types of cells are established and accepted, *in vitro* models for retinal drug delivery.

2. Materials & Methods

2.1 Materials

ARPE-19 cells were obtained from American Type Culture Collection (ATCC) and human fetal retinal pigment epithelial cells (hfRPE) were kindly donated by the National Eye Institute laboratory of Sheldon Miller Ph.D. Dulbecco's modified eagle medium (DMEM:F12 [1:1]) for cell culture, Fetal Bovine Serum, Penicillin-streptomycin antibiotic solution, PBS and mouse laminin were obtained from the UCSF Cell Culture Facility. Fetal Bovine Serum for the hfRPE cells was obtained from Atlanta Biologicals and all remaining media components were obtained from Sigma-Aldrich (Maminishkis and Miller 2006). Transwell inserts and FITC dextran spanning molecular weights of 4 to 150 kDa were obtained from Sigma-Aldrich. The hydrogel precursor solution, comprised of PEGDMA (750 mol. wt.), dimethoxy-phenyl acetophenone (DMPA) and polyvinylpyrrolidone (PVP) was purchased from Sigma-Aldrich. The SU-8 photoresist was purchased from Microchem (Newton, MA).

2.2 Cell Culture

The ARPE-19 cell line was derived from the normal eyes of a 19 year-old male. The cells were grown in a T-75 flask with a 1:1 mixture of DMEM:F12 high glucose media containing 10% Fetal Bovine Serum (FBS) and 1% Penicillin-streptomycin antibiotic solution. The *in vitro* retinal model was constructed using a 24-well, high density 0.4μm

transwell filter insert and plate assembly. The transwell filter inserts were coated with a 1:10 mouse laminin-DMEM:F12 serum free mixture and allowed to dry overnight in a cell culture hood. The ARPE-19 cells were seeded on the filters at a density of 4.5×10^5 per insert. The media used for the transwell inserts, is the same as described above with the exception of the fetal bovine serum, which is added at 1% of the total volume. All cells were maintained at 37°C in 5% CO_2. ARPE-19 cells were used between passages 25 and 35.

Passage 0 flasks were provided with hfRPE cells derived from the eyes of a 16-18 weeks of gestation fetal donor. Briefly, the cells were grown in a T-75 flask with a Minimal Essential Medium-Alpha (MEM-α) mixture of media containing 5% heat inactivated FBS, N1 supplement (1:100 mL/mL), glutamine-penicillin-streptomycin (1:100 mL/mL), nonessential amino acid solution (1:100 mL/mL), hydrocortisone (20 μg/L), tuarine (250 mg/L) and triiodo-thyronin (0.013μg/L) (Maminishkis and Miller 2006). The *in vitro* retinal model was constructed using a 24-well, high density 0.4μm transwell filter insert and plate assembly. The transwell filter inserts were coated with a human extracellular matrix from human placenta in serum free MEM-α media, UV cured for 2 hours and allowed to dry overnight in a cell culture hood. The hfRPE cells were seeded on the filters at a density of 40×10^4 per insert. All cells were maintained at 37°C in 5% CO_2. The hfRPE cells were seeded onto the inserts at passage 1 and were grown to confluence over a 6-8 week period.

2.3 Device Fabrication

The body of the microdevice was fabricated as previously described (Ainslie et al. 2009; Ainslie et al. 2008). Briefly, SU-8 was spun onto a silicon wafer and a reservoir was patterned using a two-mask photolithography process. After removal of residual photoresist with an SU-8 developer the wafer was cleaned thrice with deionized water followed by an isopropanol rinse. The wafer was then blown dry with nitrogen and baked for 2 minutes at 95°C to remove all impurities. A hydrogel solution of PEGDMA (750 mol. wt.; 2 mL) was mixed with the photoinitiator dimethoxy-phenyl acetophenone (DMPA; 200 μL of 60 mg/mL) in monomer polyvinylpyrrolidone (PVP). FITC conjugated dextran (200 μL of 20 mg/mL) of varying molecular weights was mixed with the hydrogel solution. This solution was then spun onto the SU-8 microdevice and exposed to UV-light to cross-link the hydrogel in the device reservoir.

2.4 Transport Studies

ARPE-19 and hfRPE cells were grown to confluency on porous transwell filter inserts in a 24-well plate. Confluency was measured using transepithelial electrical resistance (TEER). All transport studies were conducted on cells grown for four to eight weeks on transwell filter inserts. Equal concentrations (13 μg/mL) of the desired therapeutic (4, 40 and 150 kDa FITC dextran) were deposited in the apical chamber of the transwell filter in one of three forms: a standard bolus, a hydrogel bolus, or a planar microdevice. Cells alone and empty planar microdevices were used as controls. At periodic time points the entire volume of the basolateral chamber was removed and replaced with fresh Phosphate Buffered Saline (PBS). The samples were then probed for the concentration of FITC dextran, transferred to the basolateral chamber, using a fluorimeter. Prior to commencement of the transport studies the inserts were washed two times in PBS and transferred to a new 24-well plate. The media

was replaced with phenol red free DMEM: F12 to prevent interference with the fluorimeter measurements.

2.5 Analytical Techniques

The confluency of the ARPE-19 and hfRPE cells was measured using the World Precision Instruments transepithelial electrical resistance (TEER) device. Measurements were taken weekly until confluency was reached at approximately four and six weeks for ARPE-19 and hfRPE respectively. The concentration of FITC-conjugated agents released from the microdevice was measured with a Packard FluoroCount fluorimeter.

2.6 Immunofluorescence

ARPE-19 and hfRPE cells on transwell filter inserts were stained for the tight junction protein zonula occludens-1 (ZO-1) immediately after the conclusion of the permeability studies. The cells were fixed for 30 minutes in 4% formaldehyde-PBS solution at 4°C and washed three times with PBS. The cells were then permeabilized and blocked overnight with a 1% BSA- 0.1% Triton X solution. A ZO-1 rabbit polyclonal antibody (Invitrogen) was diluted 1:100 in blocking solution and incubated with the samples overnight at 4°C. After washing three times with PBS an Alexa Fluor secondary antibody (Invitrogen) was incubated for 1 hour at 4°C. The samples were then mounted for spinning disk confocal imaging.

2.7 qPCR for ZO-1, Occludin and MRP-1 Expression

Cell lysis, reverse transcription and quantitative polymerase chain reaction (qPCR) were performed using the Fast SYBR Green kit as outlined in the manufacturers instructions. Lysis was conducted within one hour post conclusion of the transport studies. The experiments were performed with three biological replicates (n=3) and mRNA expression was probed with three technical replicates for each respective biological replicate. The expression of GAPDH (forward 5’CTCTCTGCTCCTCCTGTTCG-3’, reverse 5’GCCCAATACGACCAAATCC-3’), ZO-1 (forward 5’TGTGAGTCCTTCAGCTGTGG-3’, reverse 5’TTTCCTGCTCAACTCCTTCG-3’), Occludin (forward 5’ACCGAATCATTATGCACCAAG-3’, reverse 5’AGATGGCAATGCACATCACAA-3’) and MRP-1 (forward 5’CTGTTTTGTTTTCGGGTTCC-3’, reverse 5’GATGGTGGACTGGATGAGGT-3’) was analyzed using the specified primer sequences. The results were normalized to GAPDH transcript levels in untreated cells using the ΔΔCt method.

2.8 MTT Assay

ARPE-19 and hfRPE cells were seeded at a density per well of 5×10^3 cells in a 96-well plate. The cells were allowed to grow for 48 hours in standard culture conditions. Both cell types were then incubated at 37°C and 5% CO_2 with and without SU-8/PEGDMA planar microdevices for 24 hours. Post incubation the cells were washed thrice with PBS to remove the planar devices. The cells were then allowed to recover for 24 hours in standard culture conditions using phenol red free media. Post recovery 20 μl of MTT solution was added to each well and incubated at 37°C for 4 hours. A volume of 200 μl of sodium dodecyl sulfate

(SDS) solubilization solution was added to the inserts post incubation. Sample absorbance was measured spectrophotometrically at 570 nm and again at 690 nm to account for the background absorbance of the 96-well plate.

2.9 Statistical Analysis

Data are reported as average values plus or minus standard deviation. All data sets were analyzed with a single factor analysis of variance (ANOVA) test followed by the Student t-test. P-values of less than 0.05 were considered statistically significant unless explicitly stated otherwise.

3. Results & Discussion

3.1 Device Characterization

Planar microdevices made with an SU-8 base and a poly(ethyleneglycol)dimethacrylate (PEGDMA) reservoir were fabricated using standard photolithography methods as outlined in figure 1a. As displayed in figure 1b, we successfully created the desired device geometry of a 150 × 150 μm base and 70 × 70 μm reservoir. We then used profilometry to verify the depth of the device reservoir and confirm that photoresist which was not crosslinked was successfully removed during the development process. Based on the desired drug loading concentration the reservoir depth was tuned to 40 micrometers as confirmed using scanning electron microscopy (Fig. S1).

Using the photolithography process flow outlined in figure 1c, FITC dextrans with a molecular weight ranging 4, 40 and 150 kDa were incorporated into a PEGDMA and photoinitiator mixture. The SU-8 patterned silicon wafer was then coated with the aforementioned hydrogel mixture using spin coating, and crosslinked in the 70 × 70 μm device reservoirs as depicted in figure 1c. Figure 1d demonstrates the successful encapsulation of the FITC labeled dextran. Corresponding elution studies confirmed that FITC dextran could be released from the devices over a four-hour period when placed in an aqueous solution (Fig. S2).

3.2 Cell Viability

The devices were incubated on the two types of retinal pigment epithelial (RPE) cells for twelve hours and cell viability was determined with the colorimetric MTT assay. ARPE-19 and hfRPE cells not exposed to planar microdevices were used as the control. The results suggested that the devices were not toxic to the cells (Fig. 2a, b). This was also confirmed via cell imaging of the ZO-1 tight junctions both with and without the presence of a device. In the absence of a device the cellular tight junctions were continuous and displayed no signs of disruption (Fig. 2c). Upon comparison to the stained cells in the presence of an empty planar microdevice one could see no significant difference in cell morphology (Fig. 2d). This supports the assertion that these devices were not toxic to RPE cells and that an adverse cellular reaction was not the cause of the increased transport witnessed in the presence of the planar microdevices.

3.3 FITC Dextran Transport Studies in ARPE-19

Figure 3 presents a schematic representation of the permeability studies experimental setup. A transwell insert with a porous membrane has been placed into a receiving chamber. The apical chamber is clearly separated from the basolateral chamber by the monolayer of retinal pigment epithelial cells (RPE). However the porous membrane, which supports the RPE cells, will permit molecules that traverse the epithelial layer to move into the basolateral chamber. In figure 3a, the apical chamber is filled with a traditional bolus of FITC dextran. This bolus was deposited using a micropipette. In figure 3b, the apical chamber is filled with FITC dextran loaded planar microdevices. The devices are removed from the wafer using a sterile razor and suspended in PBS. They are then deposited in the apical chamber using a micropipette where they settle onto the epithelial cell layer. The asymmetric design of the devices facilitates a higher concentration of FITC dextran at the epithelial cell surface.

Permeability studies using FITC dextran were conducted across a monolayer of ARPE-19 cells which were grown to confluence on the apical side of high density porous transwell inserts (qty:24, n=4) over a period of 4 to 6 weeks. These adult retinal pigment epithelial cells (ARPE-19) are the accepted *in vitro* model of the retinal epithelium (Dunn 1996; Sonoda 2009). The transport studies conducted across a monolayer of ARPE-19 cells suggested that encapsulation of FITC dextran in the planar microdevice significantly enhanced its transport compared to the traditional bolus drug deposition alone. This trend was observed for 4 kDa, 40 kDa and 150 kDa FITC dextran samples (Fig. 4a, b, c). As expected, the amount of FITC dextran transported across the monolayer of ARPE-19 cells decreased as molecular weight increased (Fig. 4d). These data suggest that planar microdevices could be of value for the delivery of biologics/proteins, which span a range of sizes, such as Insulin (6 kDa) to Bevacizumab (149 kDa). The planar architecture, unidirectional elution and increased contact time between the device and RPE cells likely contributed to the enhanced transport. Additionally, the difference in FITC dextran transported, between the device and the bolus, decreased with increasing molecular weight. This observation led us to conclude, that while these devices could be used to transport high molecular weight therapeutics, there is an upper size limit for the optimal transport effect. Additionally, this upper limit could be attributed to the hydrogel mesh size. It is well established that variations in polymer molecular weight as well as polymer and photoinitiator concentration have a direct impact on hydrogel mesh size (Hamidi et al. 2008). As a result all devices were made with PEGDMA of a single molecular weight and consistent concentrations. The mesh size of the crosslinked hydrogel is 6 to 20 nanometers in a dehydrated state. The hydrodynamic radii of the FITC dextrans used in this manuscript are 1.4, 4.5 and 8.5 nanometers and correspond to 4, 40 and 150 kDa FITC dextran respectively. The mesh size is large enough to permit diffusion of the three types of dextrans in a swollen state. However, the ratio of mesh size to hydrodynamic radius was not designed to remain constant with the increasing molecular weight of the FITC dextrans. Thus the rate of transport reduction, with increasing payload molecular weight, could also be attributed to the three distinct ratios of pore size to dextran hydrodynamic radius.

3.4 FITC Dextran Transport Studies in Human Fetal Retinal Pigment Epithelium (hfRPE)

While ARPE-19 cells are the accepted model for retinal drug transport due to their ease of acquisition and propagation, we have extended our work to a primary cell line, specifically human fetal retinal pigment epithelial cells (hfRPE). Given the morphological and physiological characteristics of hfRPE's, this culture may better mimic some of the interactions that occur *in vivo* and as such is an appropriate extension of our work. Further this primary culture has been employed to understand how well the results from our transport studies would translate to an *in vivo* model. Passage 1 of the hfRPE cells were grown to confluence on the apical side of high density porous transwell filter inserts (qty: 24, n=4) over a 6 to 8 week period. In the hfRPE experiments we observed the same trend between the hydrogel device and traditional bolus that was seen when delivering FITC dextran across ARPE-19 cells. The hydrogel-loaded microdevices outperformed the traditional bolus in the 4 kDa, 40 kDa and 150 kDa experiments (Fig. 5a, b, c). Additionally the amount of dextran transported across the hfRPE cells, decreased with the increasing molecular weight of the FITC dextran encapsulated in the hydrogel-loaded microdevices (Fig. 5d). These results have led us to conclude that our planar microdevices can be used to successfully transport large molecules across different types of retinal epithelial cells. Of greater significance is the consistent performance of the device and its drug transport across these two *in vitro* RPE models. Further this suggests that these planar microdevices could be effective in transporting therapeutics in an *in vivo* model.

To obtain additional insight into the mechanism of transport in the hfRPE experiments qPCR was conducted post drug transport experiment. Paracellular transport was considered a primary method of transport due to the large molecular weight of the FITC dextrans used in this study (Kadam et al. 2013; Mannermaa et al. 2010; Rosenthal et al. 2012). The cells were probed for expression of ZO-1 and Occludin, two tight junction proteins, which are responsible for restricting paracellular transport. It has been documented that reduced gene expression of tight junction proteins such as ZO-1 correlates with leaky tight junctions and increased permeability (Deli 2009; González-Mariscal et al. 2005). Expression of both ZO-1 and Occludin mRNA in the presence of the traditional bolus was significantly larger than all of the other delivery modes for the 40 kDa experiments (Fig. 6a). This was consistent with the 4kDa dextran experiments and supports the observed reduced transport of FITC dextran when administered via traditional bolus as compared to microdevice delivery (Fig. 5a, b, c). The hydrogel-loaded microdevice and empty device both expressed less ZO-1 and Occludin mRNA than untreated hfRPE cells. This observation led us to conclude that the devices helped facilitate transport of a 40kDa molecule via a paracellular pathway by triggering the decreased production of two tight junction proteins. Since all microdevices are cleaned, prior to contact with the cells, it is unlikely that trace chemicals from the fabrication process caused a reduction in gene expression. It is probable that direct contact between the topography of the planar device and the cell membrane initiated a signaling mechanism, which reduced tight junction gene expression (Dalby 2005; Gonzalez-Mariscal et al. 2008; Kam et al. 2013).

Based on the possibility that a mechanism other than paracellular transport could be involved, the cells were also probed for gene expression of the efflux transporter multidrug

resistance protein (MRP-1). MRP-1 has broad substrate specificity and is highly expressed in retinal cells (Constable 2008; Gunda 2008; J. Aukunuru and Kompella 2001; Mannermaa et al. 2006; Zhang et al. 2008). The traditional bolus showed a slightly decreased expression of MRP-1 mRNA as compared to the hydrogel-loaded and empty microdevices (Fig. 6b). There was however, no statistically significant difference in MRP-1 expression between the three routes of drug delivery. This suggests that MRP-1 does not play a major role in the facilitation nor hindrance of the FITC dextran transport. Combined with the ZO-1 and Occludin data, this suggests that the paracellular pathway plays a major role in the transport of FITC dextran to the basolateral chamber. This is consistent with what was expected given the size of the molecules, despite the substrate specificity of FITC to the MRP-1 efflux transporter. Building on these data, future work will target a broader set of efflux and influx transporters to understand the role they play in large molecule drug transport in the presence of planar microdevices.

4. Conclusion

A planar microdevice has successfully transported large molecules, with molecular weights of therapeutic significance, across both ARPE-19 and hfRPE cells *in vitro*. The microdevices increased the delivery of FITC dextran across an ARPE-19 and hfRPE barrier as compared to bolus administration in a molecular weight dependent fashion. This was achieved through a device triggered paracellular pathway while maintaining the integrity of the retinal cell monolayers. Further studies to understand the dominant paracellular mechanism and corresponding signaling cascade are necessary.

Supplementary Material

Refer to Web version on PubMed Central for supplementary material.

Acknowledgments

Funding to conduct this research was generously provided by Genentech, Inc and the National Institutes of Health (NIH). The hfRPE cells were generously provided by the laboratory of Dr. Sheldon Miller at the National Eye Institute (NEI). The author is grateful for the guidance on hfRPE cultivation provided by Dr. Arvydas Maminishkis of the Miller laboratory. All microfabrication work was performed in the UCSF Micro and Nanofabrication Core facility. We thank Dr. Jessica Allen, Dr. Miquella G. Chavez, Dr. Hariharasudhan D. Chirra, Dr. Osi Esue, Dr. Lalitha Muthusubramaniam and Dr. Vuk Uskokovic for their valuable insight and advice.

References

Ainslie KM, Kraning CM, Desai TA. Lab. Chip. 2008; 8:1042. [PubMed: 18584077]

Ainslie KM, Lowe RD, Beaudette TT, Petty L, Bachelder EM, Desai TA. Small. 2009; 5:2857. [PubMed: 19787677]

Anhoj TA, Jorgensen AM, Zauner DA, Hübner J. J. Micromechanics Microengineering. 2006; 16:1819.

Artursson P. Pharm. Res. 1996; 13:1686. [PubMed: 8956335]

Barar J. Expert Opin. Drug Deliv. 2008; 5:567. [PubMed: 18491982]

van Bilsen K, van Hagen PM, Bastiaans J, van Meurs JC, Missotten T, Kuijpers RW, Hooijkaas H, Dingjan GM, Baarsma GS, Dik WA. Br. J. Ophthalmol. 2011; 95:864. [PubMed: 21216798]

Booth BA, Denham LV, Bouhanik S, Jacob JT, Hill JM. Drug Aging. 2007; 24:581.

Chan AC, Carter PJ. Nat. Rev. Immunol. 2010; 10:301. [PubMed: 20414204]

Chirra HD, Desai TA. Small. 2012; 8:3839. [PubMed: 22962019]

Choonara Y. J. Pharm. Sci. 2010; 99:2219. [PubMed: 19894268]

Constable, PA. Ophthalmol. Res. Ocul. Transp. Ophthalmic Dis. Drug Deliv. Tombran-Tink, J., editor. Humana Press; Totowa: 2008. p. 235-253.

Dalby MJ. Med. Eng. Phys. 2005; 27:730. [PubMed: 15921949]

Daugherty AL, Mrsny RJ. Adv. Drug Deliv. Rev. 2006; 58:686. [PubMed: 16839640]

Deli MA. Biochim. Biophys. Acta. 2009; 1788:892. [PubMed: 18983815]

Dodane V. Int. J. Pharm. 1999; 182:21. [PubMed: 10332071]

Dornish M. Pharm. Res. 2004; 21:43. [PubMed: 14984256]

Dunn KC. Exp. Eye Res. 1996; 62:155. [PubMed: 8698076]

Edelhauser HF, Rowe-Rendleman CL, Robinson MR, Dawson DG, Chader GJ, Grossniklaus HE, Rittenhouse KD, Wilson CG, Weber DA, Kuppermann BD, Csaky KG, Olsen TW, Kompella UB, Holers VM, Hageman GS, Gilger BC, Campochiaro PA, Whitcup SM, Wong WT. Invest. Ophthalmol. Vis. Sci. 2010; 51:5403. [PubMed: 20980702]

Filpula D. Biomol. Eng. 2007; 24:201. [PubMed: 17466589]

Friedman D. Arch. Ophthalmol. 2004; 122:564. [PubMed: 15078675]

González-Mariscal L, Nava P, Hernández S. J. Membr. Biol. 2005; 207:55. [PubMed: 16477528]

Gonzalez-Mariscal L, Tapia R, Chamorro D. Biochim. Biophys. Acta. 2008; 1778:729. [PubMed: 17950242]

Gunda, S. Ophthalmol. Res. Ocul. Transp. Ophthalmic Dis. Drug Deliv. Tombran-Tink, J., editor. Humana Press; Totowa: 2008. p. 399-413.

Haghjou N, Abdekhodaie MJ, Cheng Y-L. Pharm. Res. 2012; 30:41. [PubMed: 23054085]

Hamidi M, Azadi A, Rafiei P. Adv. Drug Deliv. Rev. 2008; 60:1638. [PubMed: 18840488]

Hanrahan, F.; Campbell, M.; Nguyen, AT.; Suzuki, M.; Kiang, A-S.; Tam, LC.; Gobbo, OL.; Dhubhghaill, SN.; Humphries, MM.; Kenna, PF.; Humphries, P. Retin. Degener. Dis. LaVail, MM.; Ash, JD.; Anderson, RE.; Hollyfield, JG.; Grimm, C., editors. Springer US; Boston, MA: 2012. p. 155-159.

Hiremath JG, Devi VK. Asian J. Pharm. 2010; 4:205.

Hornof M, Toropainen E, Urtti A. Eur. J. Pharm. Biopharm. 2005; 60:207. [PubMed: 15939234]

Aukunuru J, Kompella UB. Pharm. Res. 2001; 18:565. [PubMed: 11465409]

Johnson LN, Cashman SM, Kumar-Singh R. Mol. Ther. 2007; 16:107. [PubMed: 17923842]

Kadam RS, Williams J, Tyagi P, Edelhauser HF, Kompella UB. Mol. Vis. 2013; 19:1198. [PubMed: 23734089]

Kam KR, Walsh LA, Bock SM, Koval M, Fischer KE, Ross RF, Desai TA. Nano Lett. 2013; 13:164. [PubMed: 23186530]

Kim H, Robinson SB, Csaky KG. Mol. Vis. 2009; 15:2803. [PubMed: 20019892]

Kompella UB, Amrite AC, Pacha Ravi R, Durazo SA. Prog. Retin. Eye Res. 2013; 36:172. [PubMed: 23603534]

Kompella UB, Sundaram S, Raghava S, Escobar ER. Mol. Vis. 2006; 12:1185. [PubMed: 17102798]

Kumar A, Lahiri SS, Singh H. Int. J. Pharm. 2006; 323:117. [PubMed: 16828246]

Leobandung W, Ichikawa H, Fukumori Y, Peppas NA. J. Controlled Release. 2002; 80:357.

Leobandung W, Ichikawa H, Fukumori Y, Peppas NA. J. Appl. Polym. Sci. 2003; 87:1678.

Lin JH. Curr. Drug Metab. 2009; 10:661. [PubMed: 19702530]

Maminishkis A, Miller SS. Invest. Ophthalmol. Vis. Sci. 2006; 47:3612. [PubMed: 16877436]

Mannermaa E, Reinisalo M, Ranta V-P, Vellonen K-S, Kokki H, Saarikko A, Kaarniranta K, Urtti A. Eur. J. Pharm. Sci. 2010; 40:289. [PubMed: 20385230]

Mannermaa E, Vellonen K-S, Ryhänen T, Kokkonen K, Ranta V-P, Kaarniranta K, Urtti A. Pharm. Res. 2009; 26:1785. [PubMed: 19384462]

Mannermaa E, Vellonen K-S, Urtti A. Adv. Drug Deliv. Rev. 2006; 58:1136. [PubMed: 17081648]

Mansoor S, Kuppermann BD, Kenney MC. Pharm. Res. 2009; 26:770. [PubMed: 19184374]

Mata A, Fleischman AJ, Roy S. J. Micromechanics Microengineering. 2006; 16:276.

Nirmal J, Sirohiwal A, Singh SB, Biswas NR, Thavaraj V, Azad RV, Velpandian T. Exp. Eye Res. 2013; 116:27. [PubMed: 23892056]

Paolicelli P. Expert Opin. Drug Deliv. 2009; 6:239. [PubMed: 19290841]

Peppas NA, Keys KB, Torres-Lugo M, Lowman AM. J. Controlled Release. 1999; 62:81.

Rosenthal R, Günzel D, Finger C, Krug SM, Richter JF, Schulzke J-D, Fromm M, Amasheh S. Biomaterials. 2012; 33:2791. [PubMed: 22230222]

Sonoda S. Nat. Protoc. 2009; 4:662. [PubMed: 19373231]

Tao SL, Desai TA. J. Controlled Release. 2003; 88:215.

Thrimawithana TR, Young S, Bunt CR, Green C, Alany RG. Drug Discov. Today. 2011; 16:270. [PubMed: 21167306]

Toda R, Kawazu K, Oyabu M, Miyazaki T, Kiuchi Y. J. Pharm. Sci. 2011; 100:3904. [PubMed: 21638281]

Ulery BD, Nair LS, Laurencin CT. J. Polym. Sci. Part B Polym. Phys. 2011; 49:832.

Urtti A. Invest. Ophthalmol. Vis. Sci. 2005; 46:641. [PubMed: 15671294]

Urtti A. Adv. Drug Deliv. Rev. 2006; 58:1131. [PubMed: 17097758]

Vllasaliu D. Int. J. Pharm. 2010; 400:183. [PubMed: 20727955]

Wadhwa S, Paliwal R, Paliwal SR, Vyas SP. Curr. Pharm. Des. 2009; 15:2724. [PubMed: 19689343]

Zhang T, Xiang CD, Gale D, Carreiro S, Wu EY, Zhang EY. Drug Metab. Dispos. 2008; 36:1300. [PubMed: 18411399]

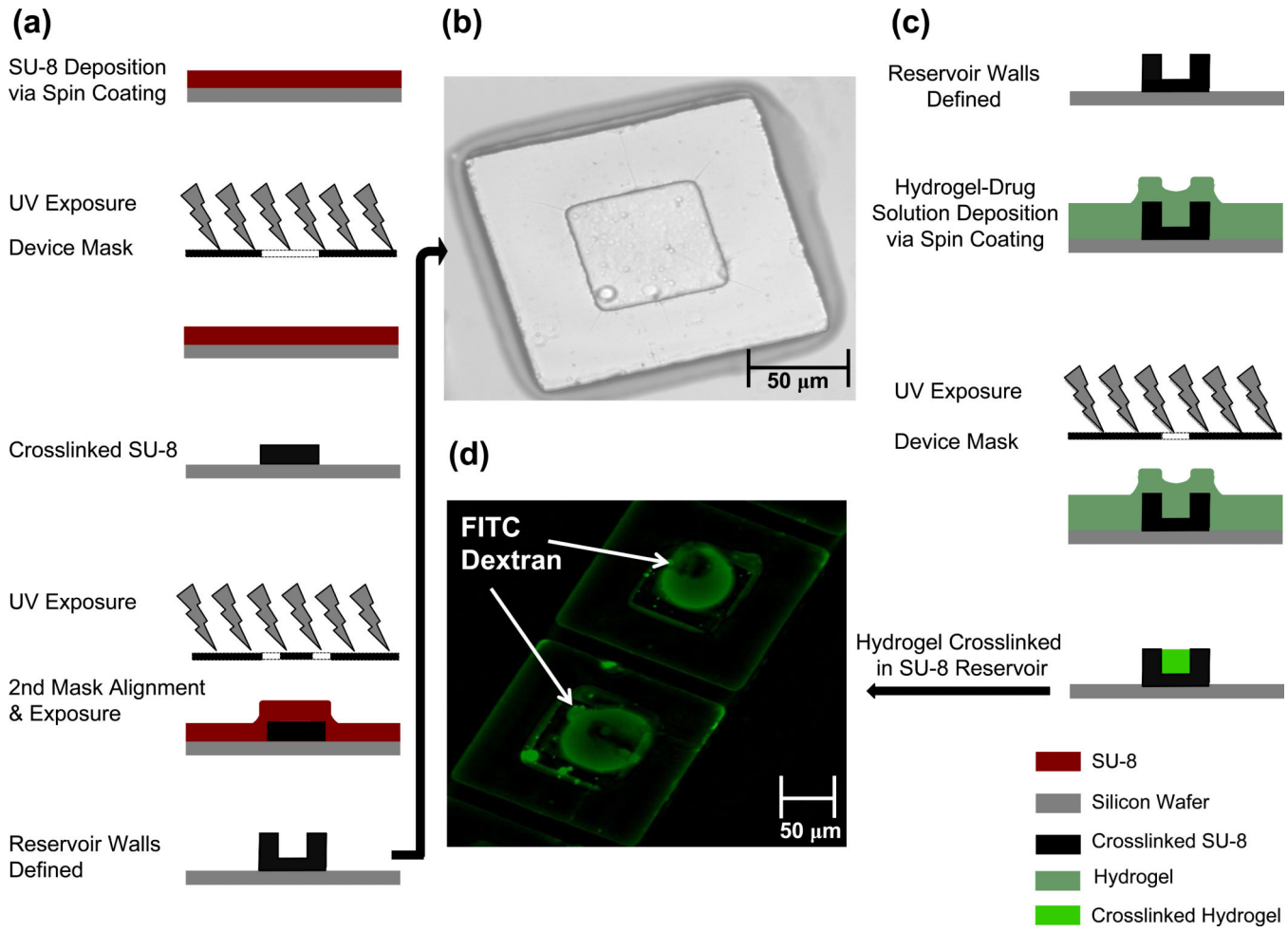

Fig. 1.

SU-8 Device Fabrication Process and PEGDMA Hydrogel Encapsulation. (a) Schematic representation of fabrication using standard photolithography and a two-mask process to generate a reservoir structure. (b) Bright field image of SU-8 device with defined features. (c) Schematic representation of PEGDMA Hydrogel being crosslinked in the device reservoir (d) Image of encapsulated FITC conjugated drug [4 kDa dextran]

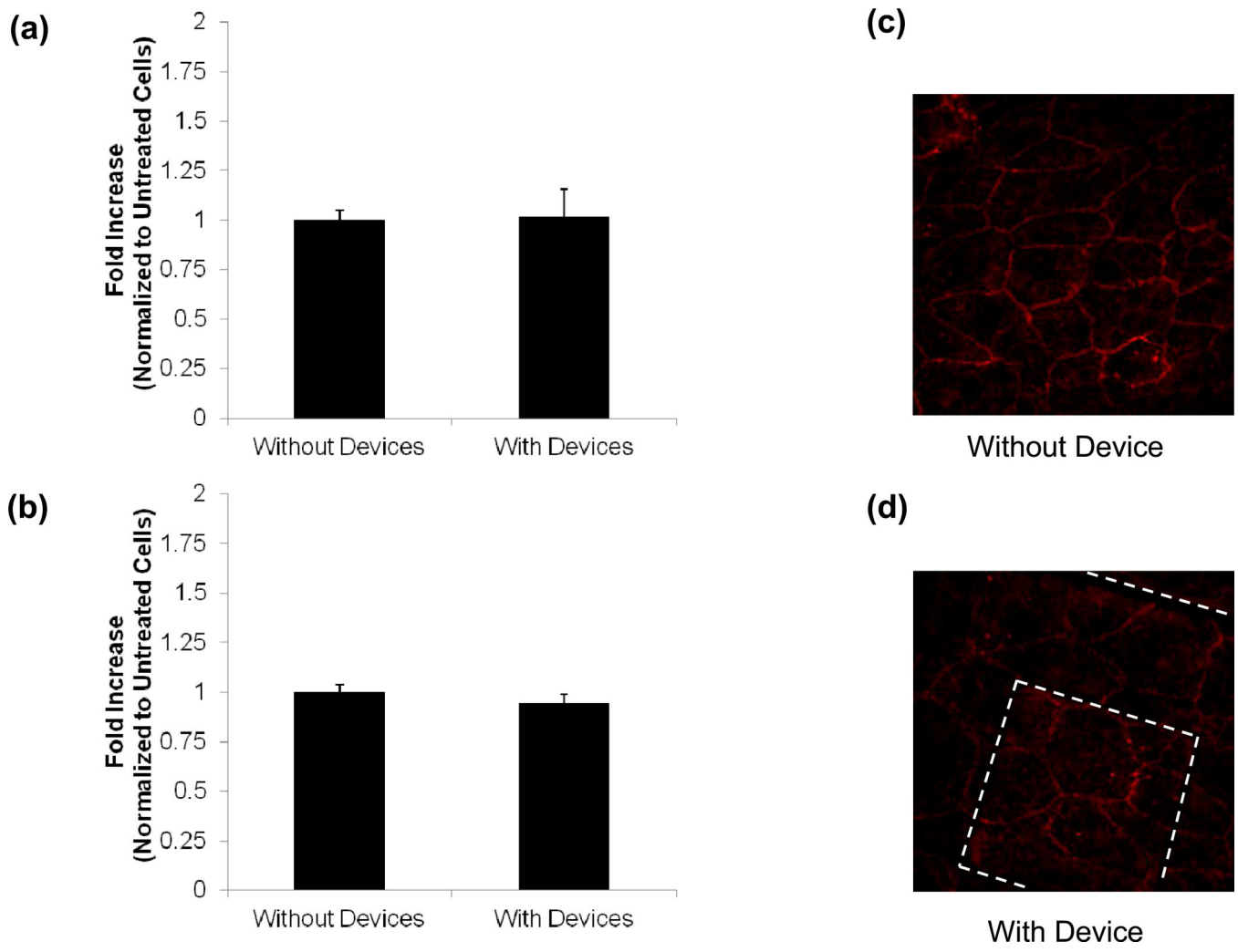

Fig. 2.

MTT Assay. MTT assay of (a) ARPE-19 and (b) hfRPE incubation with and without devices confirms cell viability. ARPE-19 zonula occludens 1 (ZO-1) staining confirms formation of tight junctions (c) without devices and (d) with devices. All data is presented as +/- standard deviation. An asterisk (*) indicates statistical significance with respect to the untreated cells with a P-value of less than 0.05

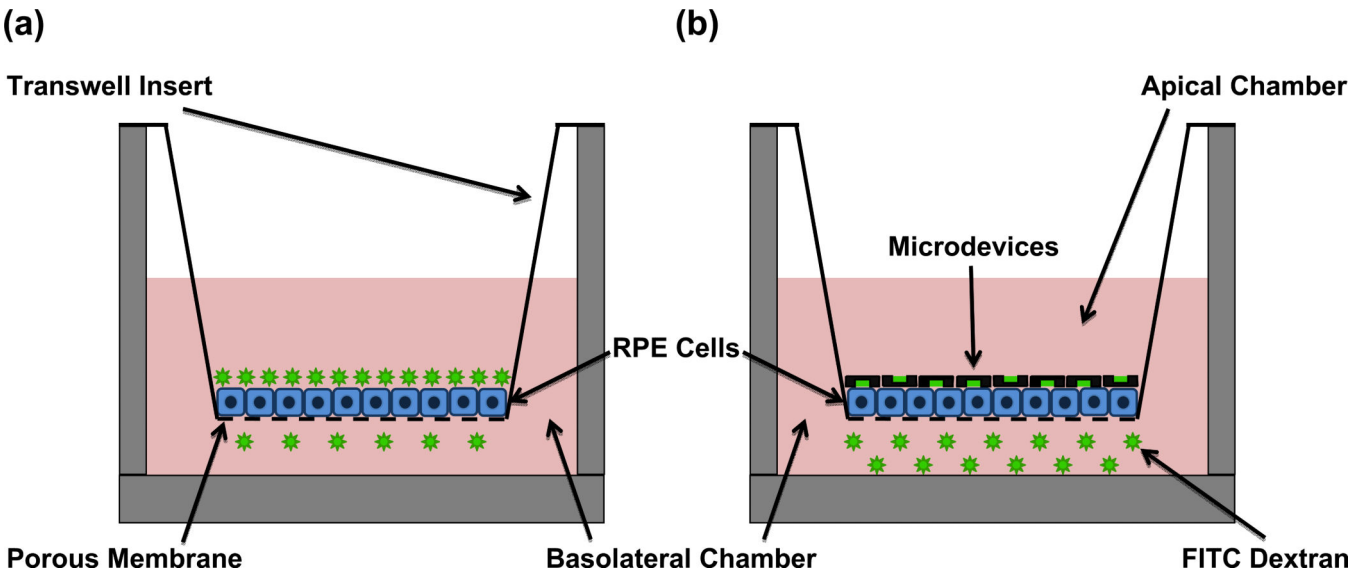

Fig. 3.

Permeability Studies Experimental Setup. (a) Schematic representation of a transwell insert with bolus drug being deposited in the apical chamber. (b) Schematic representation of drug loaded SU-8/PEGDMA planar microdevices being deposited in the apical chamber of a transwell insert

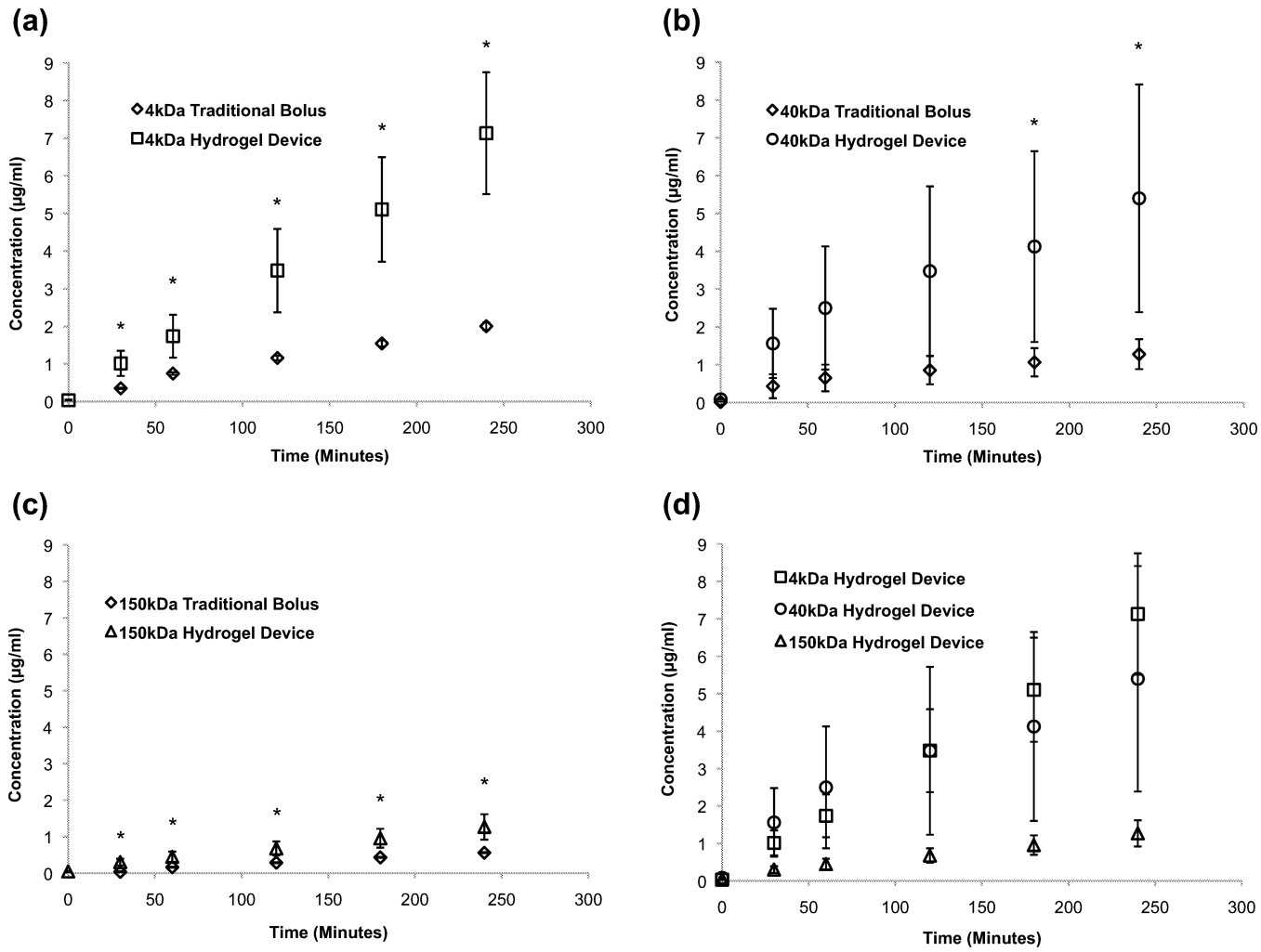

Fig. 4.

ARPE-19 Permeability Studies. Transport of FITC dextran across a monolayer of ARPE-19 cells grown on transwell inserts using a traditional bolus and planar hydrogel devices. FITC dextran of varying molecular weights (a) 4 kDa, (b) 40 kDa, (c) 150 kDa was deposited in the apical chamber and encapsulated in planar SU-8/PEDGMA devices for each experiment. (d) The concentration of drug transported is molecular weight dependent. An asterisk (*) indicates statistical significance with respect to the traditional bolus conditions. All data is presented as +/- standard deviation

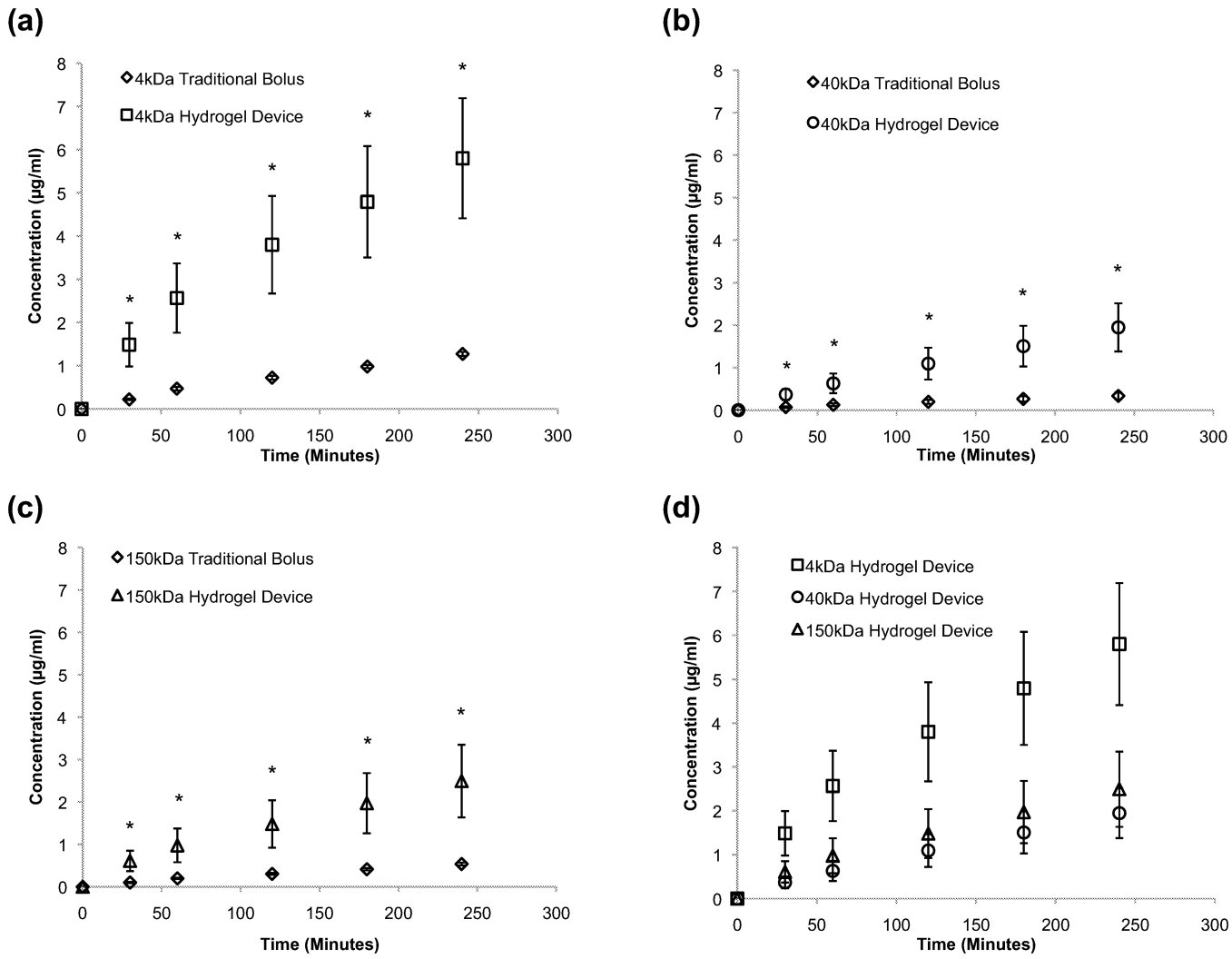

Fig. 5.

hfRPE Permeability Studies. Transport of FITC dextran across a monolayer of hfRPE cells grown on transwell inserts using a traditional bolus and planar hydrogel devices. FITC dextran of varying molecular weights (a) 4 kDa, (b) 40 kDa, (c) 150 kDa was deposited in the apical chamber and encapsulated in the uncoated planar SU-8/PEDGMA devices for each experiment. (d) The concentration of drug transported is molecular weight dependent. An asterisk (*) indicates statistical significance with respect to the traditional bolus conditions. All data is presented as +/- standard deviation

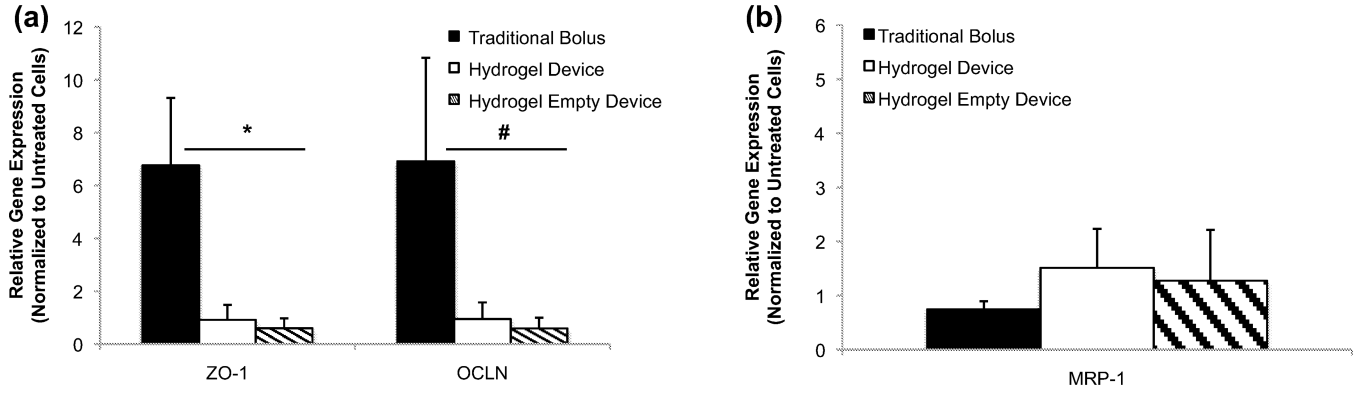

Fig. 6.

Quantitative PCR Studies (hfRPE). Relative gene expression of (a) tight junction proteins post planar microdevice permeability study [40 kDa FITC dextran]. (b) Relative gene expression of MRP-1 efflux transporter protein post planar microdevice permeability study [40 kDa FITC dextran]. All data is normalized by the gene expression of the control (untreated cells) and presented as mean +/- standard deviation. An asterisk (*) indicates statistical significance with respect to the traditional bolus of less than 0.05 and a hash mark (#) indicates statistical significance with respect to the traditional bolus of less than 0.07